North American Power Symposium (NAPS), Cleveland, Ohio, October 1998.

Multi-parameter Bifurcation Analysis of Power Systems

André A. P. Lerm
Dept. Electrical Engineering
Fed. Univ. of Santa Catarina
88040-900, Florianópolis, SC
Brazil
alerm@labspot.ufsc.br

Claudio A. Cañizares
E&CE Department
University of Waterloo
Waterloo, ON, N2L-3G1
Canada
c.canizares@ece.uwaterloo.ca

Flávio A. B. Lemos
Dept. Electrical Engineering
Fed. Univ. of Santa Catarina
88040-900, Florianópolis, SC
Brazil
flavio@labspot.ufsc.br

Aguinaldo S. e Silva
Dept. of Electrical Engineering
Fed. Univ. of Santa Catarina
88040-900, Florianópolis, SC
Brazil
aguinald@labspot.ufsc.br

***Abstract*—This paper presents a detailed bifurcation analysis of multi-parameter power systems. Equilibrium points are used to evaluate the system eigenvalues and obtain different bifurcation diagrams for two sample systems. The paper studies the influence of hard-limits, AVR droop and reactive power compensation on the local bifurcations of the test systems, using detailed generator models. The stability regions of equilibrium points and the effect that various bifurcations have on them are also studied.**

Keywords: Voltage stability, modal analysis, bifurcation diagrams, stability regions, limits, reactive power compensation.

1. INTRODUCTION

Various types of stability problems in power systems, such as voltage collapse and oscillatory phenomena, can be analyzed through bifurcation theory [1]. Thus, bifurcation analysis has become an important analysis tool in stability studies of these systems. This paper presents a practical and detailed study of different test systems, to show the influence of various system parameters, control limits and settings in the bifurcation analysis and stability of realistic power systems.

Typically, the bifurcations associated with different stability problems are local bifurcations, and hence they can be studied through the eigenvalues of the linearization around an operating point of the differential-algebraic equations (DAE) used to model the system. These equilibria are typically obtained from load flow analysis, due to the simplicity of its formulation, obtaining a variety of operating points as certain system parameters change (usually the load). These points are then used to create the well-known power/voltage or PV curves, where various stability regions are identified based on the results of the eigenvalue studies. Although in some particular cases PV curves may represent bifurcation diagrams [2], in most practical cases that is not the case [3]. Thus, the authors in [3] and [4] show that there are other implicit independent parameters that must be taken into account to qualify the stability regions on the PV curves obtained via a conventional load flow. For example, a generator is assumed to have a constant terminal voltage in the load flow model; however, if the corresponding AVR is modeled in detail, the voltage set-point for this controller must change at each point on the PV curve to account for voltage droop, and hence keep the terminal voltage constant. Thus, in this case, the problem requires a multi-parameter bifurcation analysis, as shown here for two different test systems.

A fairly comprehensive summary of the various types of bifurcations that can be encountered in power systems models is presented in [5]. In this paper, the authors present a complete taxonomy of the different stability regions of large dynamical systems. They consider that the parameter space is composed by *typal regions* (regions of structural stability) bounded by bifurcation surfaces; these surfaces are determined by different kinds of bifurcations, such as saddle-nodes, Hopfs, singularity induced bifurcations and limit induced bifurcations. The latter, in particular, are due to controller limits in the system, and were studied through transcritical bifurcations in [6] to show the effect of generator reactive power limits on system stability. A couple of test systems are used in [7] to illustrate the regions of stability as defined by some of these bifurcations on the PV curves.

In [8] the authors study, based on transient energy functions, the effect of saddle-node bifurcations on the stability regions of power system equilibria, showing that as the system approaches the saddle-node, the stability region decreases until it becomes "zero" at the saddle-node, i.e., the perturbations that the system can withstand decrease as the system approaches the bifurcation point. The author in [9] uses also energy functions to show how shunt and series reactive power compensation affect these stability regions. The energy function technique cannot be used to study the effect on the stability regions of bifurcations where equilibrium points do not merge (e.g., Hopfs); hence, the current paper illustrates the effect of these bifurcations on stability using actual time domain simulations of a given perturbation, so that relative sizes of the system stability regions can be determined.

This paper first describes the basic characteristics of all these local bifurcations for a generic system model, to then proceed to illustrate the effect that different parameters and limits have on the bifurcations and stability regions of practical system models. Thus, this paper is organized as follows: Section 2 briefly discusses some of the theoretical foundations of bifurcation analysis of power systems, using as an example a 3-busbar system to show the typical behavior of different bifurcation manifolds when controller droops and limits are considered. Section 3 presents the complete

bifurcation analysis of a 39-busbar test system, demonstrating the effect of reactive power compensation on the corresponding bifurcation diagrams and the system stability regions. Finally, Section 4 presents the main conclusions of this paper.

2. Bifurcation Analysis

Nonlinear dynamical systems, such as those obtained from certain power system models, can be generically described by the following ordinary differential equations (ODE):

$$\dot{x} = f(x, \lambda, p) \tag{1}$$

where $x \in \Re^n$ corresponds to the state variables; $\lambda \in \Re^l$ represents a particular set of "non-controllable" scalar parameters that drive the system to a bifurcation in a quasi-static manner, i.e., as λ changes, the system steadily moves from equilibrium point to equilibrium point; $p \in \Re^k$ represents a series of "controllable" parameters associated with control settings; and $f: \Re^n \times \Re^l \times \Re^k \rightarrow \Re^n$ is a nonlinear vector function.

Typical power system models used in stability analysis present an additional difficulty, as these systems are modeled with a set of differential and algebraic equations (DAE) of the form

$$\begin{bmatrix} \dot{x} \\ 0 \end{bmatrix} = \begin{bmatrix} f(x, y, \lambda, p) \\ g(x, y, \lambda, p) \end{bmatrix} = F(z, \lambda, p) \tag{2}$$

where $x \in \Re^n$ typically stands for state variables corresponding to a series of system devices, such as generators, and their controls; $\lambda \in \Re^l$ stands for slow varying parameters that are typically associated with changing loading levels, over which operators have no direct control; $p \in \Re^k$ represents the control settings that operators directly or indirectly control, such as AVR reference set-points or shunt compensation; $f: \Re^n \times \Re^m \times \Re^l \times \Re^k \rightarrow \Re^n$ corresponds to the nonlinear vector field directly associated with the state variables x; the vector $y \in \Re^m$ represents the set of algebraic variables defined by the nonlinear algebraic function $g: \Re^n \times \Re^m \times \Re^l \times \Re^k \rightarrow \Re^m$ which typically correspond to load bus voltages and angles, depending on the load models used; and $F = (f,g)$ and $z = (x,y)$.

The stability of DAE systems is thoroughly discussed in [10]. The main idea in that paper is that if $D_y g(x,y,\lambda,p)$ can be guaranteed to be nonsingular along system trajectories of interest, the behavior of system (2) along these trajectories is primarily determined by the local ODE reduction

$$\dot{x} = f(x, y^{-1}(x, \lambda, p), \lambda, p)$$

where $y = y^{-1}(x,\lambda,p)$ comes from applying the Implicit Function Theorem to the algebraic constraints $g(x,y,\lambda,p)=0$ on the trajectories of interest. Equilibrium points of (2), i.e., $F(z_o,\lambda_o,p_o) = 0$, where $D_y g|_o$ is singular are known as singularity induced (SI) bifurcation points [5],[11], and are characterized by an eigenvalue of the Jacobian matrix

$$A = D_x f|_o - D_y f|_o \left[D_y g|_o\right]^{-1} D_x g|_o) \tag{3}$$

changing from $+\infty$ to $-\infty$, or vice versa.

A. Equilibria and Steady-state Operating Points

An issue that one must be aware of in stability analysis is that system equilibria obtained from $F(z_o,\lambda_o,p_o) = 0$ are typically defined through a subset of equations typically referred to as the load flow equations,

$$G(z'_o, \lambda_o, p'_o) = G|_o = 0 \subset F(z_o, \lambda_o, p_o) = F|_o = 0$$

where z' and p' are also subsets of z and p, respectively. Hence, the typical procedure is to first solve the load flow equations and, based on the corresponding solutions, find equilibrium points of the dynamic model before proceeding with stability analysis of the full dynamic system of equations (2). For some particular dynamic F and load flow G models, all load flow solutions may correspond to actual system equilibria and vice versa [12]. However, for most realistic dynamic and load flow models, the solution of the load flow equations does not guarantee an initial system equilibria, as solutions of $G|_o = 0$ do not necessarily guarantee that $F|_o = 0$ exists, and vice versa; this is particularly important for the discussions regarding bifurcation diagrams in the following sections.

Even when the proper system equilibria are available, i.e., equilibrium points are computed from system equations (2), AVR set-points, which typically form part of the controllable parameter set p, must be allowed to change in order to model constant generator terminal voltages, which is standard steady-state operating procedure. In other words, some of the parameters p must be interchanged with some of the z variables, solving $F(z'_o,\lambda_o,p'_o) = 0$ to obtain the desired operating points.

B. Local Bifurcations

Standard bifurcation theory deals with the study of the stability of ODE systems (1) that move from equilibrium to equilibrium as the parameters λ slowly change [13],[14]; these bifurcation concepts can be directly extended to DAE systems represented by (2) [2],[15]. There are several types of bifurcations associated with the changes of λ, some are local and some are global, depending on the behavior of the system dynamic manifolds and equilibrium points. The current paper concentrates only on the analysis of local bifurcations, which can be detected and analyzed by monitoring the eigenvalues of the system Jacobian (3). The following is a list of the generic, local bifurcation that are most likely to be encountered in power systems:

- *Node Focus (NF)*: These types of bifurcation are characterized by a complex conjugate pair of eigenvalues merging into one real eigenvalue, or vice versa, as the parameters λ change slowly. Although there is no significant change on the stability of the system, these bifurcations seem to be precursors to other types of bifurcations [7].

- *Saddle-node (SN)*: These bifurcations, also known as turning points or fold bifurcations, are typically identified by a couple of equilibrium points merging at the bifurcation point and then locally disappearing as the slow varying parameters λ change. Many cases of actual voltage collapse in power systems have been associated with saddle-node bifurcations. This bifurcation corresponds to an equilibrium point (z_o,λ_o,p_o) where the system Jacobian A defined in (3) has a unique zero eigenvalue, and certain transversality conditions, which distinguish it from other types of "singular" bifurcations (transcritical and pitchfork), are met [16].
- *Hopf (HP)*: These bifurcations are characterized by a complex conjugate pair of eigenvalues crossing the imaginary axes of the complex plane from left to right, or vice versa, as the λ parameters slowly change. These types of bifurcations have been associated with a variety of oscillatory phenomena in power systems [1], and are typical precursors of chaotic motions [13],[14].
- *Singularity Induced (SI)*: These bifurcations, as previously explained, are due to a singularity of the algebraic equations' Jacobian $D_y g|_o$, and correspond to equilibrium points where an eigenvalue of the system Jacobian A defined in (3) changes from +/-∞ to -/+∞.
- *Limit Induced (LI)*: These bifurcations correspond to equilibrium points where system limits are reached as the parameters λ slowly change, with the corresponding eigenvalues undergoing instantaneous changes that may affect the stability status of the system, such as stable eigenvalues turning into unstable ones [5].

C. Example

In this section, the previous theory is used to study load changes in the hypothetical 3-busbar test system shown in Fig. 1. One of the generators is assumed to be an infinite bus, and the other generator is modeled using 5 differential equations (2 for the mechanical dynamics, 3 for the transient dynamics), plus a simple AVR with droop, and no governor. Changes in the active power demand are picked up by the infinite bus. The data for this system is shown in Table I.

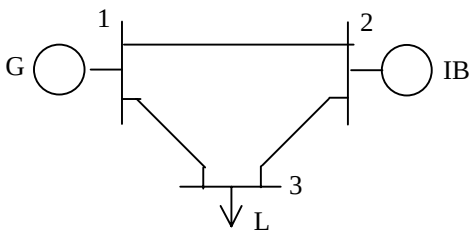

Fig. 1. Three-bus sample system.

TABLE I
P.U. DATA FOR 3-BUS SAMPLE SYSTEM.

H	10.0 s	τ'_{do}	8.5 s	P_{lo}	0.8
X_d	0.9	τ''_{do}	0.03 s	Q_{lo}	0.6
X_q	0.8	τ''_{qo}	0.9 s	V_{t2}	1.0
X'_d	0.12	P_m	1.0	$X_{1\text{-}2}$	0.2
X''_d	0.08	K_{AVR}	50.0	$X_{2\text{-}3}$	0.2
X''_q	0.08	T_{AVR}	0.5 s	$X_{1\text{-}3}$	0.2

In spite of the size of this system, the qualitative results obtained for it extend to large real power systems. All simulations are carried out modeling the load as static constant power, with the bifurcation parameter λ representing the active and reactive power load changes at bus 3 as follows: $P_l = P_{lo}(1+\lambda)$, $Q_l = Q_{lo}(1+\lambda)$; where P_{lo} and Q_{lo} are the initial values shown in Table I. In this case, the AVR reference set-point V_{ref} corresponds to the controllable parameter p.

To analyze the influence of limits on the bifurcation diagrams, results are first obtained for the case with no limits on E_{fd}, and then compared to the case where limits are considered. In both cases, V_{ref} is varied within a relatively wide range of values to study its effect on the system bifurcations.

1) Case without limits: The results obtained in this case are shown in Figs. 2 and 3, where the voltage at bus 3 V_3 is plotted as function of V_{ref} and λ. Figure 3 is just a projection and zoom-in of Fig. 2. For each value of V_{ref} one can observe that the system has 4 basic bifurcations. Thus, the system first becomes unstable through a Hopf bifurcation, as showed by the line HP; this bifurcation is then followed by a node focus (NF), singularity induced (SI) and saddle-node (SN) bifurcations, in that order. The Hopf bifurcation occurs when a complex conjugate pair of stable eigenvalues crosses over the imaginary axis, from left to right. At the node focus bifurcation, the complex pair of unstable eigenvalues changes to two real eigenvalues in the right-hand side of the complex plane (unstable node focus). One of the positive real eigenvalues then moves to the left-hand side through a singularity induced bifurcation from -∞ to +∞, while the other eigenvalue becomes zero at the saddle-node bifurcation, which corresponds to the point of maximum power transfer for this particular DAE system.

In both of these figures, a dashed line represents the solutions to the load flow problem as λ changes. It is important to indicate that the load flow used to obtain the results depicted in this paper models accurately the limits on the generators' AVR [17]. This line, which basically represents the PV curve, is obtained by assuming a fixed generator terminal voltage, allowing V_{ref} to change accordingly.

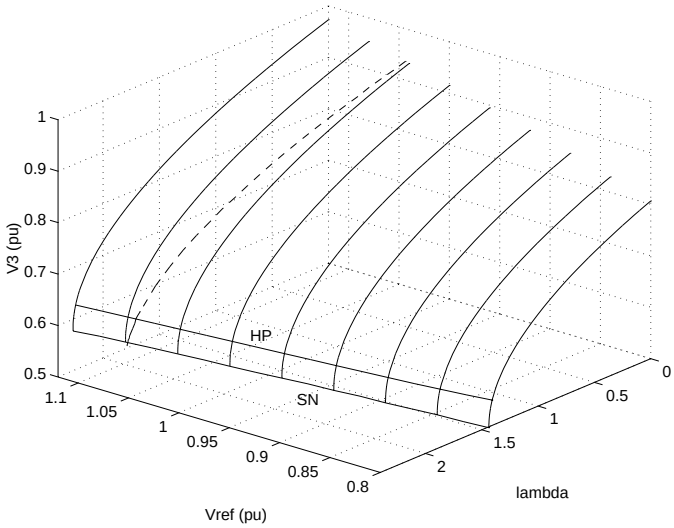

Fig. 2. Bifurcation diagram for 3-bus test system without limits.

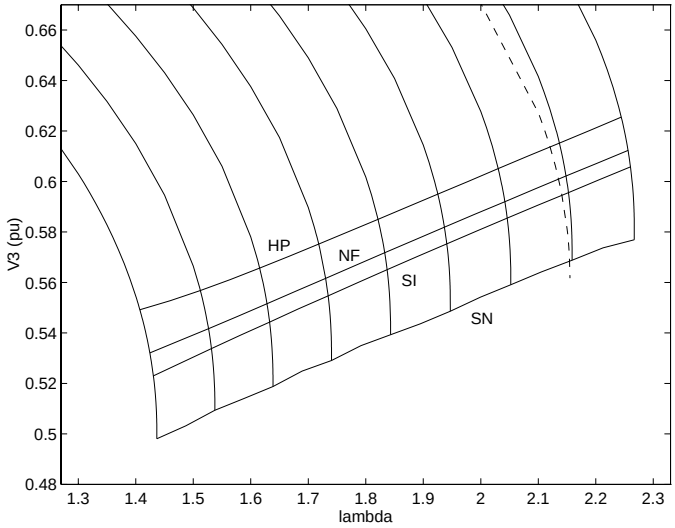

Fig. 3. Projection of the bifurcation diagram for 3-bus test system without limits.

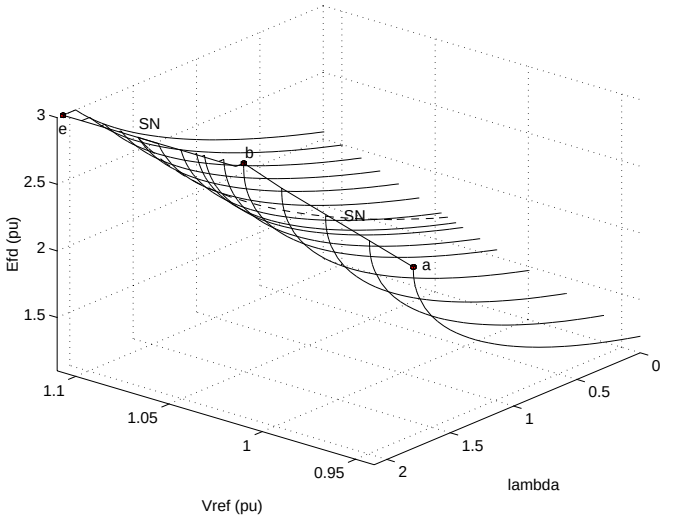

Fig. 4. Bifurcation diagram for 3-bus test system with E_{fd} limits.

2) Case with limits: Hard limits of ±3.0 p.u. on the field voltage E_{fd} are added in this case to the AVR model. Figure 4 shows the behavior of E_{fd} versus V_{ref} and λ up to the saddle-node (SN) bifurcation; no other bifurcations are depicted in this diagram to avoid cluttering up the picture. Figure 5 depicts V_3 versus the parameters V_{ref} and λ, plus some of the other bifurcations that occur "before" the saddle-node. The generator does not reach a limit until the set-point V_{ref} attains a value of 1.0172 (point b on the curves). Hence, the bifurcation diagrams are basically the same as in the case with no limits, up to this V_{ref} value, with saddle-nodes occurring at points on the a-b section.

The two dimensional diagram of Fig. 6 is used here to explain the effect of the different parameters and limits on the system bifurcations. On this figure one can observe that when $1.0173<V_{ref}<1.0355$, the system first experiences a Hopf, then a node focus and finally a singularity induced bifurcation (SI1) as λ changes, like in the case without limits. However, when the generator reaches its E_{fd} limit (point b), there is an immediate change in stability and then the system follows a new stable bifurcation manifold (between points b and a second singularity induced bifurcation SI2). This turning point is also referred to as a limit induced (LI) bifurcation.

For V_{ref} values between 1.0355 and 1.0392 the bifurcation diagram first reaches a Hopf and then a node focus, followed by a limit induced bifurcation. At this point, one of the two positive real eigenvalues originated by the node focus immediately moves to the left-hand side of the complex plane, while the remaining positive eigenvalue moves towards zero at the saddle-node bifurcation. This phenomenon occurs until V_{ref} = 1.0393, when the NF manifold disappears.

For $1.0393<V_{ref}<1.0471$ the system initially experiences the Hopf and then the limit induced bifurcation (line c-d). The latter immediately undoes the unstable complex pair created by the Hopf, yielding two new real eigenvalues, one positive and another negative. The positive one eventually approaches zero at the saddle-node bifurcation. The Hopf manifold disappears at V_{ref} = 1.0471; thus, for $V_{ref}>1.0471$ there is only a limit induced bifurcation, and a saddle-node point. This limit induced bifurcation forces a negative eigenvalue to become immediately positive, and hence the system becomes immediately unstable when the generator reaches its limits.

Finally, for $V_{ref}>1.0590$, the system experiences a stable limit induced bifurcation, similar to a stable node focus, before the saddle-node bifurcation point. Observe that for $V_{ref}<1.0173$ there is an a-b line of saddle-node bifurcation points; however, for $V_{ref} \geq 1.0173$ there is only one saddle-node bifurcation point.

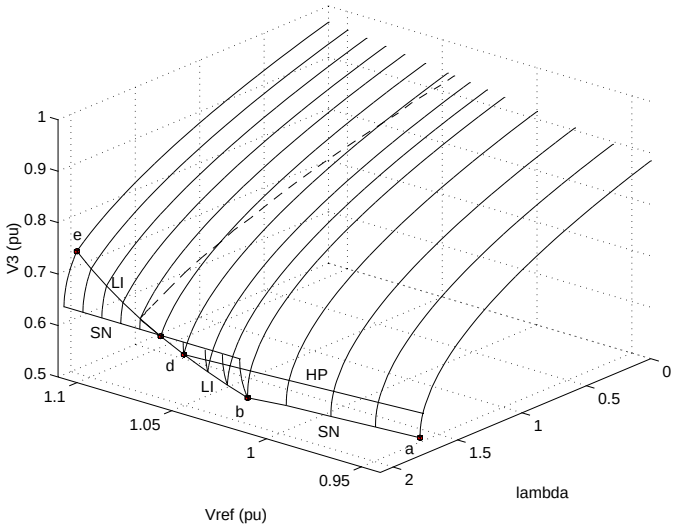

Fig. 5. Bifurcation diagram for 3-bus test system with limits (V_3).

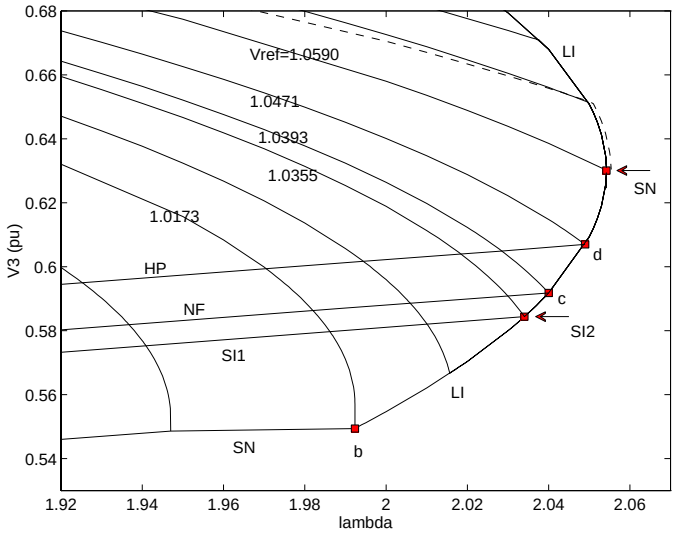

Fig. 6. Projection of the bifurcation diagram for 3-bus test system with limits.

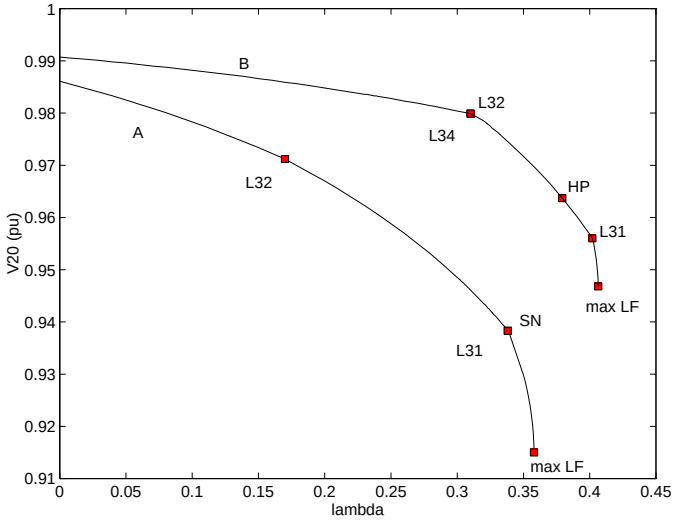

Fig. 7. Bifurcation diagram for 39-bus New England test system.

3. Practical Applications

The previous section discussed the use of bifurcation theory to study the stability of the operating points of a small system, showing the influence of AVR droops and limits on the bifurcation diagrams. In this section, a similar approach is followed to study the bifurcation of the 39-bus New England system. However, the equilibrium points in this case are only obtained from the load flow equations with accurate representation of the AVR limits.

The realistic, detailed model of the New England test system presented in [18] is used here to demonstrate the influence of reactive power compensation on power system bifurcations. The bifurcation parameter λ is used again to model constant power load variations in all buses, i.e., $P_l = P_{lo}(1+\lambda)$ and $Q_l = Q_{lo}(1+\lambda)$, where P_{lo} and Q_{lo} are the initial values for the loads. The loads are modeled as static constant power loads, and machine #39 is assumed to be the swing bus; all limits are modeled as hard limits. In order to obtain more interesting results, the original E_{fd} limits of all generators are reduced by 25%.

A. Original System

The bifurcation study results for this case are shown on Fig. 7, curve A. Generator #34 is at its Q limits at the base load ($\lambda = 0$), while generators #32 and #31 reach their limits at points L32 ($\lambda = 0.16954$) and L31 ($\lambda = 0.33724$), respectively. Each limit point corresponds to a limit induced bifurcation with a complex conjugate pair of eigenvalues becoming real (similar to a node focus bifurcation), and instability occurs at $\lambda = 0.33819$ through a saddle-node bifurcation (point SN). It must be noticed that the maximum loading for the load flow occurs at $\lambda = 0.35795$, well after the system has become unstable; this is typical of stability studies that compute initial conditions from a conventional load flow routine, which is common practice in industry.

B. With Reactive Power Compensation

For this study, reactive power shunt-compensation of 103.9, 103.1 and 73.3 Mvar is allocated at buses 31, 32 and 34, respectively. This compensation corresponds to 50% of the reactive power generated at these buses for the base case ($\lambda = 0$). With this compensation, generators 34, 32 and 31 reach their limits at $\lambda = 0.31457$, 0.30747, and 0.40229, respectively (points L34, L32 and L31 on curve B, Fig. 7). As in the previous case, at these points the system experiences limit induced bifurcations similar to stable node focus bifurcations. The instability occurs in this case at $\lambda = 0.37928$ through a Hopf bifurcation (point HP); no saddle-node is detected.

An analysis of these results reveals the significant influence of reactive power compensation on the system bifurcations. Although not all detailed bifurcation diagrams are shown for this system due to their complexity, it is easy to observe that the manifold of equilibrium points derived from

the load flow intercepts the saddle-node and Hopf manifolds in different ways, depending on the reactive power compensation levels. This is particularly important when designing reactive power compensation of power systems, which is the preferred way nowadays to increase transmission system capability.

C. *Stability Regions*

Figure 8 depicts the relative size of the stability region of the test system before (SN) and after compensation (HP). These plots were obtained by determining, through time domain simulations, the largest instantaneous load change in all buses (plotted on the vertical axis in p.u.) that the system can withstand before becoming unstable; this test gives a true sense of the size of the stability region without the need for any of the approximations required when using energy functions. Observe that the system becomes more stable by adding reactive power compensation, as it is to be expected [9]. In both cases the stability region decreases as λ increases, reaching a "zero" value at the saddle-node or Hopf bifurcation points, respectively. It is interesting to notice that the system bifurcating through a Hopf shows a more rapid reduction of the stability region as λ changes.

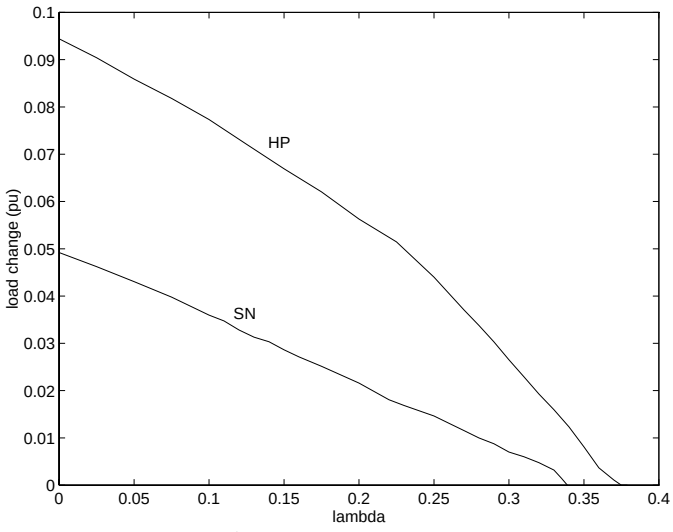

Fig. 8. Stability region for the 39-bus New England test system.

4. Conclusions

The paper presents a thorough bifurcation analysis of detailed power system models, showing the effect of different control parameters and limits on the bifurcation and associated stability behavior of the system. The issue of using conventional load flows versus the actual equilibrium equations to compute equilibrium points for bifurcation analysis is also discussed in detail.

This paper concentrates on showing the practical applications of bifurcation theory, and its stability implications for realistic power systems. The main idea here is to apply the current extensive bifurcation theoretical background to practical systems; thus, the next step is to continue with similar studies for a real model of the Brazilian power system.

5. Acknowledgment

The authors gratefully acknowledge the financial support of the Brazilian Government agency CAPES. The authors also acknowledge the support of Pontifícia Universidade Católica do Rio do Grande do Sul, Universidade Católica de Pelotas, Escola Técnica Federal de Pelotas, and the Natural Science and Engineering Research Council (NSERC) of Canada.

References

[1] P. Kundur, ed., "Voltage Stability Assessment, Procedures and Guides," IEEE/PES Power System Stability Subcommittee Special Publication, Final Draft, July 1998, http://www.power.uwaterloo.ca

[2] C. A. Cañizares, "Conditions for saddle-node bifurcations in AC/DC power Systems," *Int. J. of Electric Power & Energy Systems*, vol. 17, no. 1, pp. 61-68, Feb. 1995.

[3] B. C. Lesieutre, P. W. Sauer, and M. A. Pai, "Why Power/Voltage Curves Are Not Necessarily Bifurcation Diagrams," *25th North American Power Symposium*, Washington, pp. 30-37, Oct. 1993.

[4] M. A. Pai, P. W. Sauer, and B. C. Lesieutre, "Static and Dynamic Nonlinear Loads and Structural Stability in Power Systems," *Proceedings of the IEEE*, vol. 83, pp. 1562-1572, Nov. 1995.

[5] V. Venkatasubramanian, H. Schättler, and J. Zaborszky, "Dynamics of Large Constrained Nonlinear Systems–A Taxonomy," *Proceedings of the IEEE*, vol. 83, pp. 1530-1561, Nov. 1995.

[6] I. Dobson and L. Lu, "Immediate Change in Stability and Voltage Collapse When Generator Reactive Power Limits are Encountered," *Proceedings of Bulk–Power Voltage Phenomena II – Voltage Stability and Security*, Maryland, pp. 65-73, Aug. 1991.

[7] B. Lee and V. Ajjarapu, "A Piecewise Global Small-disturbance Voltage-stability Analysis of Structure-preserving Power System Models", *IEEE Transactions on Power Systems*, vol. 10, no. 4, pp. 1963-1971, Nov. 1995.

[8] T. J. Overbye and C. L. DeMarco, "Voltage Security Enhancement Using Energy Based Sensitivities," *IEEE Transactions on Power Systems*, vol. 6, no. 3, pp. 1196-1202, Aug. 1991.

[9] C. A. Cañizares, "Calculating Optimal System Parameters to Maximize the Distance to Saddle-node Bifurcations," *IEEE*

Trans. Circuits and Systems–I, vol. 45, no. 3, pp. 225-237, March 1998.

[10] D. J. Hill and I. M. Y. Mareels, "Stability Theory for Differential/Algebraic Systems with Application to Power Systems," *IEEE Trans. Circuits and Systems*, vol. 37, no. 11, pp. 1416-1423, Nov. 1990.

[11] V. Venkatasubramanian, H. Schattler, and J. Zaborszky, "A Taxonomy of the Dynamics of the Large Power Systems with Emphasis on its Voltage Stability," *Proc. Bulk Power System Voltage Phenomena II–Voltage Stability and Security*, ECC Inc., pp. 9-52, Aug. 1991.

[12] I. Dobson, "The irrelevance of load dynamics for the loading margin to voltage collapse and its sensitivities," *Proc. Bulk Power System Voltage Phenomena III–Voltage Stability and Security*, ECC Inc., pp. 509-518, Aug. 1994.

[13] R. Seydel, *Practical Bifurcation and Stability Analysis–From Equilibrium to Chaos*, Second Edition, Springer-Verlag, New York, 1994.

[14] J. Guckenheimer and P. Holmes, *Nonlinear Oscillations, Dynamical Systems and Bifurcation of Vector Fields*. Applied Mathematical Sciences, Springer-Verlag, New York, 1986.

[15] H. G. Kwatny, R. F. Fischl, and C. O. Nwankpa, "Local Bifurcation in Power Systems: Theory, Computation, and Application," *Proceedings of the IEEE*, vol. 83, pp. 1456-1483, Nov. 1995.

[16] C. A. Cañizares and S. Hranilovic, "Transcritical and Hopf Bifurcations in AC/DC Systems," *Proc. Bulk Power System Voltage Phenomena III–Voltage Stability and Security*, ECC Inc., pp. 105-114, Aug. 1994.

[17] A. A. P. Lerm, F. A. B. Lemos, A. S. e Silva, and M. Irving, "Voltage Stability Assessment with Inclusion of Hard Limits," accepted for the *Proc. of the IEE*, Feb. 1998.

[18] "Frequency Domain Analysis of Low Frequency Oscillations in Large Electric Power Systems," Interim Report El-726, EPRI, 1978.

André Arthur Perleberg Lerm received his degree in Electrical Engineering from Universidade Católica de Pelotas, Brazil in 1986, and the M.Sc. degree in Electrical Engineering from Universidade Federal de Santa Catarina, Brazil in 1995. He is currently a Ph.D. student at Universidade Federal de Santa Catarina, in a joint split Ph.D. program with the University of Waterloo, Canada. Since 1987 and 1988, he has been with Universidade Católica de Pelotas and Escola Técnica Federal de Pelotas, respectively. His main research interests are in the area of power systems dynamics, voltage stability and systems modeling.

Claudio A. Cañizares received the Electrical Engineer diploma (1984) from the Escuela Politécnica Nacional (EPN), Quito-Ecuador, where he held different positions from 1983 to 1993. His M.Sc. (1988) and Ph.D. (1991) degrees in Electrical Engineering are from the University of Wisconsin-Madison. Dr. Cañizares is currently an Associate Professor at the University of Waterloo and his research activities are mostly concentrated on the study of computational, modeling, and stability issues in ac/dc/FACTS power systems.

Flávio Antônio Becon Lemos received his degree in Electrical Engineering from Universidade Federal de Santa Maria, Brazil in 1988, and the M.Sc. degree in Electrical Engineering from Universidade Federal de Santa Catarina in 1994. He is currently a Ph.D. student at Universidade Federal de Santa Catarina. He was employed by CEEE, RS from 1989 to 1991. Since 1990, he has been with Pontifícia Universidade Católica do Rio Grande do Sul, Porto Alegre, Brazil. His main research interests are in the area of power systems dynamics, voltage stability and non-linear systems.

Aguinaldo Silveira e Silva received his degree in Electrical Engineering from the Universidade Federal de Parana, Brazil in 1977, and the M.Sc. and Ph.D. degrees in Electrical Engineering from Universidade Federal de Santa Catarina, Brazil, in 1982 and UMIST, UK, in 1990, respectively. Since 1980, he has been with the Universidade Federal de Santa Catarina. His main research interests are in the area of power systems dynamics and control applications.